

# The retinoic acid receptor co-factor NRIP1 is uniquely upregulated and represents a therapeutic target in acute myeloid leukemia with chromosome 3q rearrangements

Sarah Grasedieck,<sup>1</sup> Ariene Cabantog,<sup>2</sup> Liam MacPhee,<sup>2</sup> Junbum Im,<sup>2</sup> Christoph Ruess,<sup>3</sup> Burcu Demir,<sup>3</sup> Nadine Sperb,<sup>3</sup> Frank G. Rucker,<sup>3</sup> Konstanze Döhner,<sup>3</sup> Tobias Herold,<sup>4</sup> Jonathan R. Pollack,<sup>5</sup> Lars Bullinger,<sup>6</sup> Arefeh Rouhi<sup>2#</sup> and Florian Kuchenbauer<sup>2#</sup>

<sup>1</sup>University of British Columbia, Department of Microbiology & Immunology, Vancouver, British Columbia, Canada; <sup>2</sup>Terry Fox Laboratory, BC Cancer Agency, Vancouver, British Columbia, Canada; <sup>3</sup>Ulm University Hospital, Department of Internal Medicine III, Ulm, Germany; <sup>4</sup>Department of Medicine III, University Hospital, LMU Munich, Munich, Germany; <sup>5</sup>Department of Pathology, Stanford University School of Medicine, Stanford, CA, USA and <sup>6</sup>Department of Hematology, Oncology and Tumor Immunology, Charité University Medicine, Berlin, Germany.

*#AR and FK contributed equally as co-senior authors.*

## Correspondence:


Florian Kuchenbauer  
[fkuchenbauer@bccrc.ca](mailto:fkuchenbauer@bccrc.ca)

**Received:** November 16, 2020.

**Accepted:** November 25, 2021.

**Prepublished:** December 2, 2021.

<https://doi.org/10.3324/haematol.2020.276048>

©2022 Ferrata Storti Foundation  
Haematologica material is published under  
a CC-BY-NC license 

**Content:**

- **Supplementary Figure Legends.**
- **Supplementary Figures S1 to S11.**
- **Supplementary Methods.**

**Figure S1. A)** TPM-normalized *LOC101927745* and *NRIP1* expression in four sorted human hematopoietic progenitor populations: CD34<sup>+</sup>/lin<sup>-</sup>, granulocytic precursors (GMP), monocytic precursors (MDP), and erythrocytic precursors (MEP) obtained from MDS patient and healthy donor BM (RNAseq, GEO ID: GSE114922). *p*-values were calculated comparing the individual groups to “all samples”, using the Welch Two Sample *t*-test adjusted for multiple hypothesis testing. **B)** Expression of *LOC101927745* and *NRIP1* determined via qRT-PCR (n=3 biological and n=3 technical replicates) in the histiocytic lymphoma U937, the secondary erythroleukemia HEL, the chronic myeloid leukemia K562, the acute promyelocytic leukemia NB-4 and in 11 AML cell lines relative to *ABL1* and *SDHC* housekeeping genes. Delta Ct values (gene of interest – housekeeping gene) were subtracted from the value 40, corresponding to the number of PCR amplification cycles. Therefore, higher values correspond to higher gene expression and an overall comparison of relative transcript abundance among individual cell lines is possible. **C)** Group fold changes calculated as 2<sup>ΔΔCt</sup> (EVI1<sup>low</sup> – EVI1<sup>high</sup>) and scatterplot showing the correlation of *LOC101927745* and *NRIP1* transcript expression based on data from B. **D)** Expression of *NRIP1* and EVI1 in a microarray dataset from EVI1<sup>low</sup> and EVI1<sup>high</sup> expressing AML cell lines (GEO accession ID: GSE35159). All *p*-values were calculated using the Welch Two Sample *t*-test.

**Figure S2.** Results from Univariate Cox Proportional Hazard (CoxPH) analyses and graphical representation of Kaplan-Meier estimates based on *EVI1* (*MECOM*), *NRIP1*, and *LOC101927745* transcript levels calculated in the adult AML subset of the Beat AML Master Trial cohort<sup>16</sup>, retaining all patients with available survival information. The same analysis was performed with step-wise, leave-one-out removal of indicated cytogenetic patient subgroups and expression cut-offs were kept constant. *P*-values were calculated using the log-rank test.

**Figure S3. A)** Chromatin interactions mapped through ChIA-PET and ChIP-seq tracks for CTCF and cohesin (Rad21). ChIA-PET cluster data was generated in Gm12878 (GEO ID: GSE72816) and K562 (GEO ID: GSM970216) cells, ChIP-seq data for CTCF and Rad21 in K562 (GEO ID: GSE32465) and THP-1 AML cell lines (GEO ID: GSE55407). Blue lines mark Ctf-bound sites with a significant physical interaction score. **B)** ChIP-seq tracks (2 replicates per track) showing murine Ctf in E14 cells (GEO ID: GSE136488) and murine Rad21 in immortalized B10 cells (GEO ID: GSE36030). **C)** UCSC genome browser snapshot showing species conservation of the *NRIP1* and *LOC101927745* genomic region in indicated vertebrates. **D)** *LOC101927745* sequence (NCBI BLAST alignment highlighted in red) and orientation towards its neighboring genes are conserved in the mouse genome.

**Figure S4. A)** UCSC genome browser shot indicating the CRISPR/Cas9-deleted region annotated as *LOC101927745* TSS, exon1, and part of exon 2 in the human genome version hg38. Shown tracks depict NCBI RefSeq genes including predicted transcripts (release 109.20190905), layered H3K27 acetylation (ENCODE<sup>24</sup>), GeneHancer<sup>38</sup>-listed regulatory elements and predicted interactions, and DNase I hypersensitive sites (ENCODE<sup>24</sup>). **B)** UCSC genome browser view of H3K27me3 (top), H3K9me3 (middle) and input control (bottom). ChIPseq signal density in four primary AML CD34<sup>+</sup> blast samples from the BLUEPRINT epigenome project<sup>17</sup> at the *LOC101927745* and *NRIP1* locus. Data was mapped to human genome version hg38 and is available at <https://epigenomesportal.ca/ihec/>. **C)** PCR products from annotated *LOC101927745* exons 1 and 2 (within the CRISPR/Cas9-deleted region) with cDNA reverse-transcribed from DNase-digested RNA obtained from OCI-AML-5 *LOC101927745*

knockout (LOC KO) and empty control vector-transduced cells following single cell clone sorting and expansion.

**Figure S5.** ATRA- and TPA-induced morphologic changes in the OCI-AML5 *LOC101927745*-KO and empty vector carrying *LOC101927745*-WT cell lines. Clonally expanded cell lines treated with either 0.1 $\mu$ M ATRA (DMSO) or 5nM TPA in 3 independent rounds of experiments. **A)** Before treatment as well as after 24 and 48 hours of treatment, cytopspins were prepared, stained with May-Grünwald/Giemsa and images were taken at 60x magnification. Representative images from each condition are shown. **B)** ITGAX/CD11c mature myeloid cell surface marker expression of *LOC101927745*-KO and *LOC101927745*-WT control cell lines during drug induced *in vitro* differentiation. ITGAX was stained and expression quantified via flow cytometry before (baseline / d0), after 24h and after 48h of ATRA or TPA treatment, respectively. *P*-values were calculated using a paired, two-tailed Student's t-test for unequal variance.

**Figure S6.** ChIP-seq footprinting data **A)** for RUNX1, EVI1 and GATA-2, which together form an abnormal transcription-activating complex in t(3;21)(q26;q22) SKH1 AML cells and **B)** UCSC genome browser shot showing gene annotations and the "TFBS Conserved" data track (last updated: 2011-03-06) containing the location and score of transcription factor binding sites conserved in the human/mouse/rat alignment. Binding sites were considered to be conserved across the alignment if their scores met the precomputed default z-score threshold of 2.33 in all 3 species. All scores and thresholds were computed with the Transfac Matrix Database (v7.0) created by Biobase. Sites highlighted in yellow represent conserved binding sites for the EVI1 transcription factor. The red box indicates the location of the putative *NRIP1* enhancer *GH21J015439* within the *LOC101927745* TSS.

**Figure S7.** Chromosome 3 intact OCI-AML3, Kasumi-1 and K562 cells were lentivirally transduced with constructs encoding either *NRIP1*-targeting or two different control shRNAs in 3 independent experiments. Puromycin-selected cells were seeded at 0.25x10<sup>6</sup> cells/mL and either treated with 0.5 $\mu$ M ATRA or DMSO control and a total of 3 replicates per condition were harvested and analyzed after 24h and 72h. **A)** Cells were resuspended, stained with Trypan blue and counted at the indicated time points. Shown is the total number of Trypan-negative (live) cells per well over time. **B)** Cells were stained with Annexin-V and Sytox at the indicated time points and 10,000 cells per sample were recorded via flow cytometry. Shown are % Annexin/Sytox double negative (i.e. non-apoptotic) cells relative to d0 of the experiment. **C)** RNA was extracted from 3 individual treatment samples per condition, DNase-digested and reverse-transcribed to cDNA. In the same sample, RNA levels of *NRIP1*, *EVI1* (*MECOM*), and the housekeeping gene *ABL1* were quantified using commercially available TaqMan assays in technical triplicates. Transcript levels of *LOC101927745* (exon 1) were quantified using SYBR Green chemistry and compared to the housekeeping gene *SDHC*. Fold changes were calculated using the 2<sup>ddCt</sup> method with sh-contr. samples set to 1.

**Figure S8 and S9.** Total protein was extracted, BSA-quantified and Western blots were performed with *NRIP1*- and  $\beta$ -Actin targeting antibodies from three individually generated cell lines per condition. Signal intensity of *NRIP1*- relative to  $\beta$ -Actin bands was quantified using Fiji/Image J. All shown *p*-values were calculated using paired, two-tailed Student's *t*-tests for unequal variance.

**Figure S10.** Alternative analysis of the qRT-PCR data recorded as a downstream analysis of the experiment described in **Figure 6** in the indicated cell lines and conditions. Depicted plots show data obtained by subtracting individually calculated deltaCt (dCt) values from the arbitrarily chosen value 40, corresponding to the number of PCR reactions. dCt values still retain a logarithmic nature, therefore bar heights in the depicted plots underrepresent the actual fold changes in expression. However, this representation allows to compare the relative abundancy among different RNA transcripts and treatment conditions, e.g. within the same cell line over time. Expression differences in sh-contr. and sh-*NRIP1*-expressing cells lines in response to ATRA or DMSO treatment were assessed. Unpaired two-tailed Student's *t*-test for samples with unequal variance was used to assess statistical significance of the observed changes.

**Figure S11.** Chromosome 3 normal OCI-AML3 cells and t(3;3) UCSD-AML1 cells were transfected with *NRIP1*-targeting or negB control GapmeRs in 3 independent experiments, seeded at  $0.5 \times 10^6$  cells/mL and either treated with  $0.5 \mu\text{M}$  ATRA or DMSO control. After 24h, a total of 3 replicates per condition were harvested and analyzed for cell proliferation and apoptosis. **A)** Cells were resuspended, stained with Trypan blue and counted at the indicated time points. Shown is the % increase in cell number within 24 hours. Only Trypan-negative (live) cells were considered. **B)** Cells were stained with Annexin-V-APC and Sytox Blue and 10,000 cells per sample were recorded via flow cytometry. Shown are % Annexin/PI double negative (non-apoptotic) cells. **C)** RNA was extracted, DNase-digested and reverse-transcribed to cDNA from experimental triplicates of the indicated cell lines. RNA levels of *NRIP1* and the housekeeping gene *ABL1* were quantified using commercially available TaqMan assays. Fold changes were calculated using the  $2^{\text{ddCt}}$  method with sh-contr. samples set to 1. **D)**  $0.5 \times 10^6$  *EVI1*<sup>high</sup> expressing t(3;3) UCSD-AML1 cells/mL were treated in 2 independent sets of experiments with either two different *NRIP1*-targeting FAM-labeled antisense GapmeRs, 6 different *LOC101927745*-targeting GapmeRs, a non-target control (negB) or with transfection agent alone (lipofectamin). Cell growth was assessed 24h post treatment and growth rates calculated as described in the methods section. *P*-values were calculated using the Welch Two Sample *t*-test.

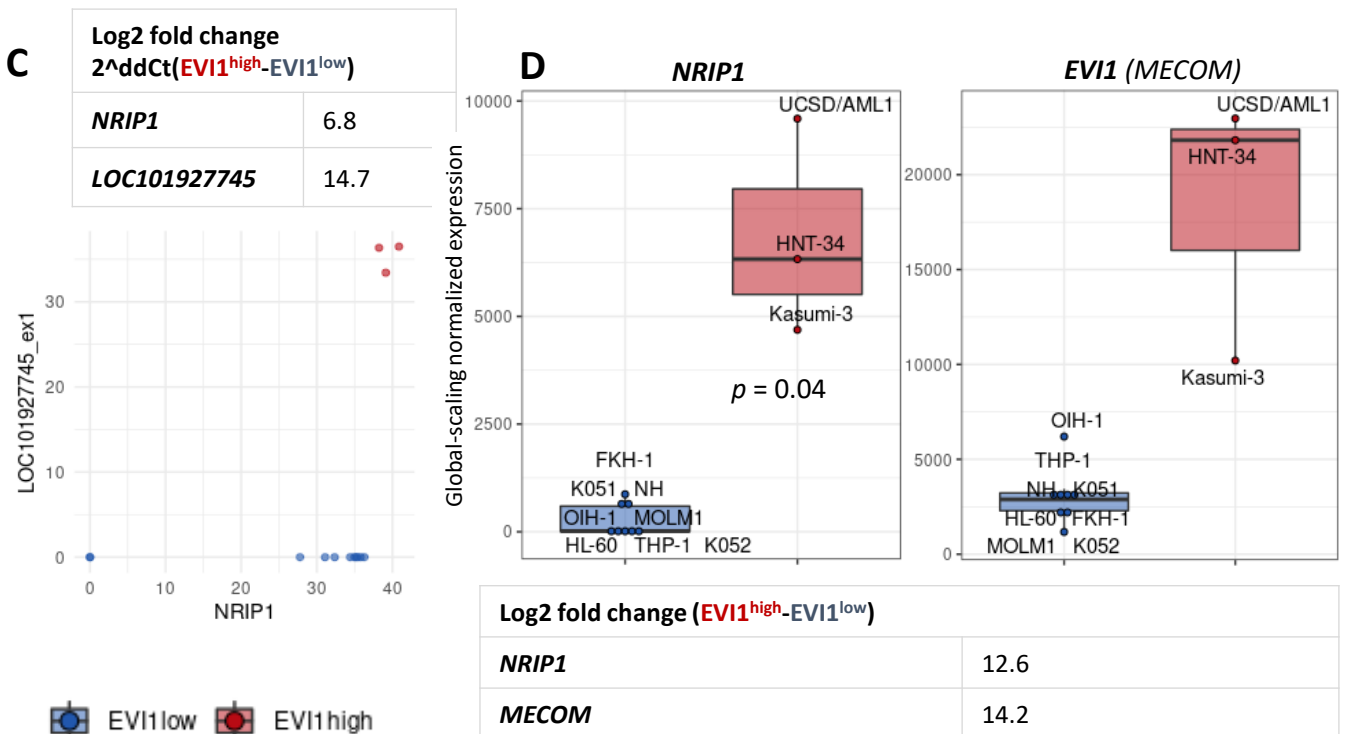
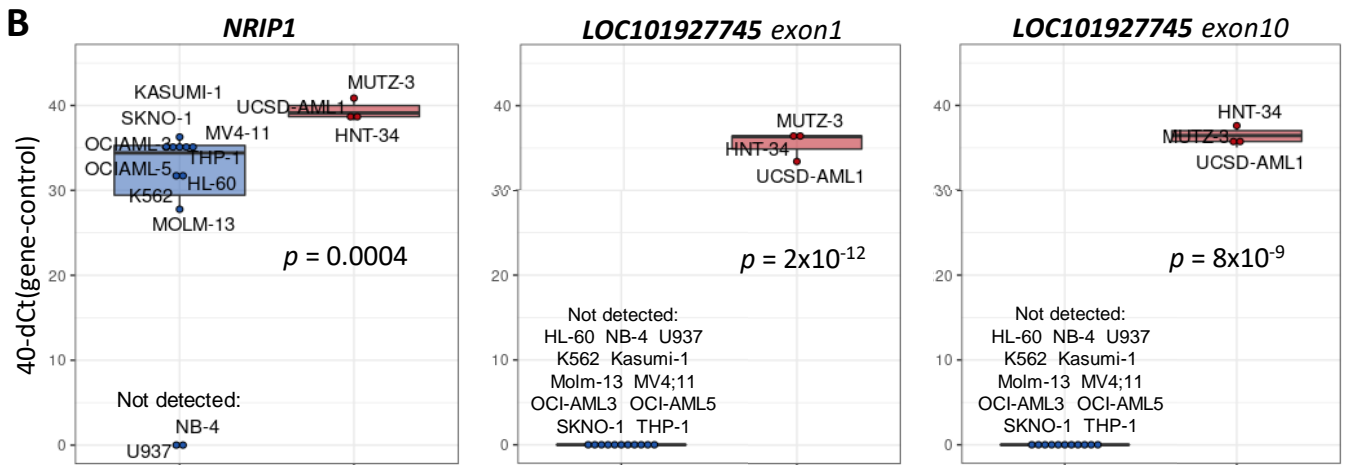
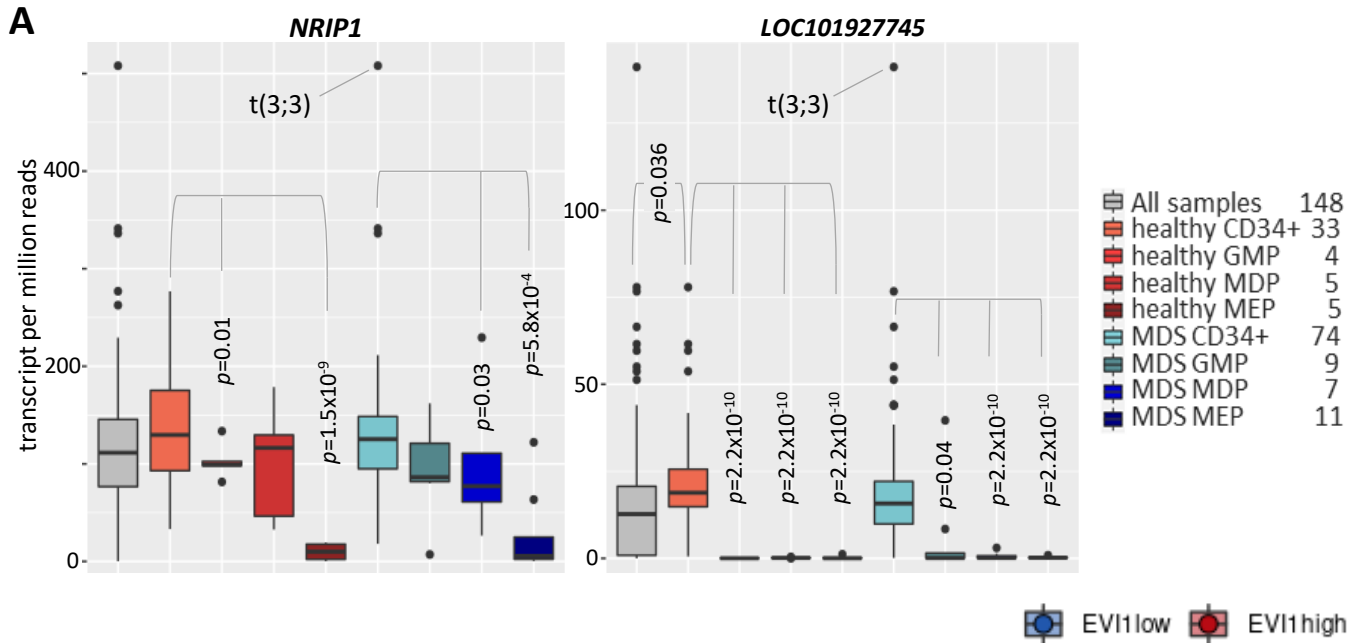


Figure S1.

<b>Hazard ratio (univariate CoxPH)</b>	BeatAML all cases	BeatAML no inv(3)	BeatAML no inv(3), CK	BeatAML no inv(3), CK, del(7)/del(5)
<i>LOC101927745</i>	2.19	2.96	2.38	2.35
<i>NRIP1</i>	3.54	3.73	3	3.04
<i>EVI1/MECOM</i>	0.997	0.34	0.39	0.36
Patient age	6.6	6.69	6.45	6.41

<b>corresponding <i>p</i>-values</b>	BeatAML all cases	BeatAML no inv(3)	BeatAML no inv(3), CK	BeatAML no inv(3), CK, del(7)/del(5)
<i>LOC101927745</i>	0.028	0.003	0.017	0.018
<i>NRIP1</i>	0.0004	0.0002	0.002	0.002
<i>EVI1/MECOM</i>	0.319	0.736	0.695	0.718
Patient age	4.13e-11	2.24e-11	1.09e-10	1.44e-10

n =	451	436	392	386
-----	-----	-----	-----	-----

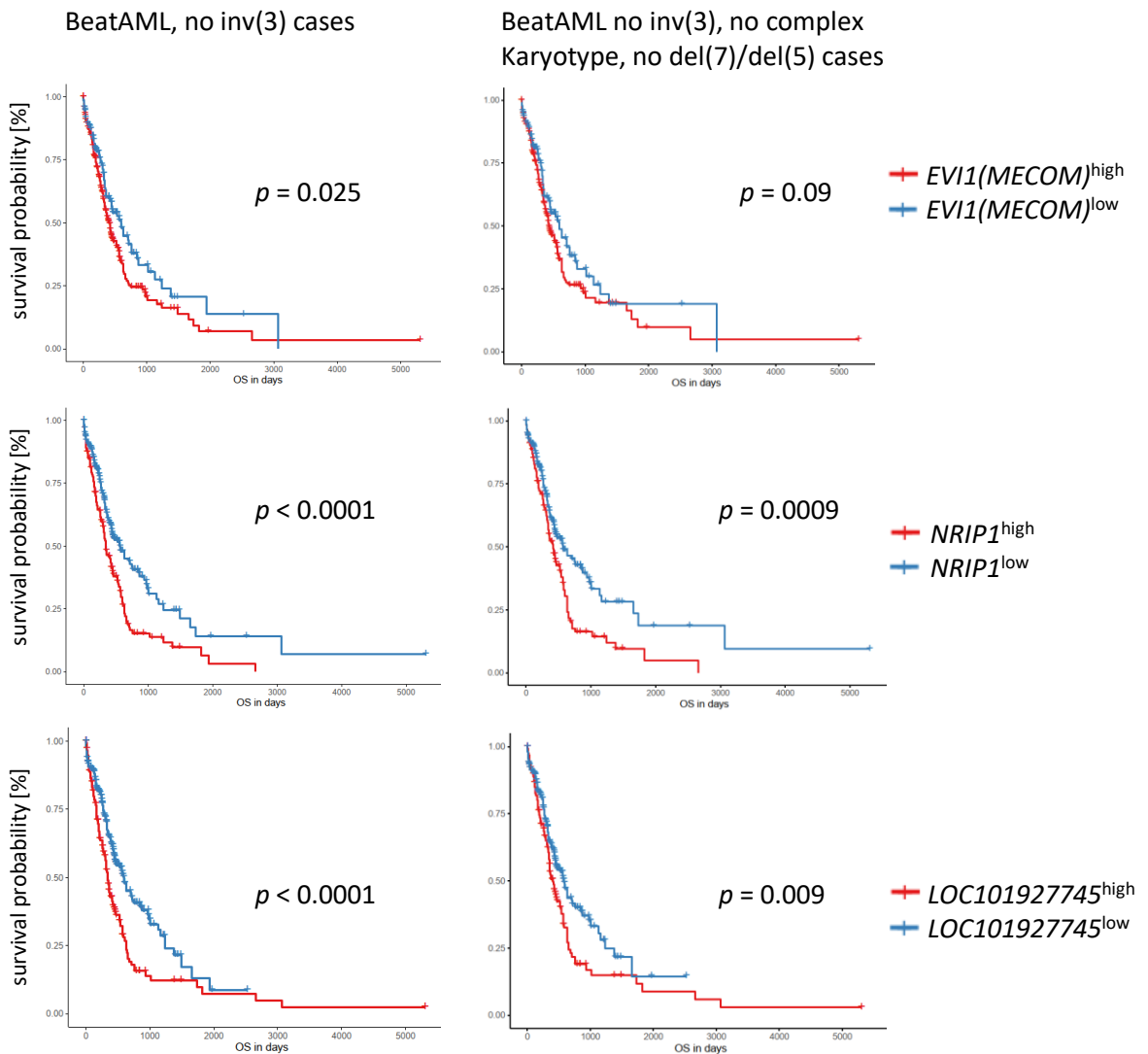


Figure S2.

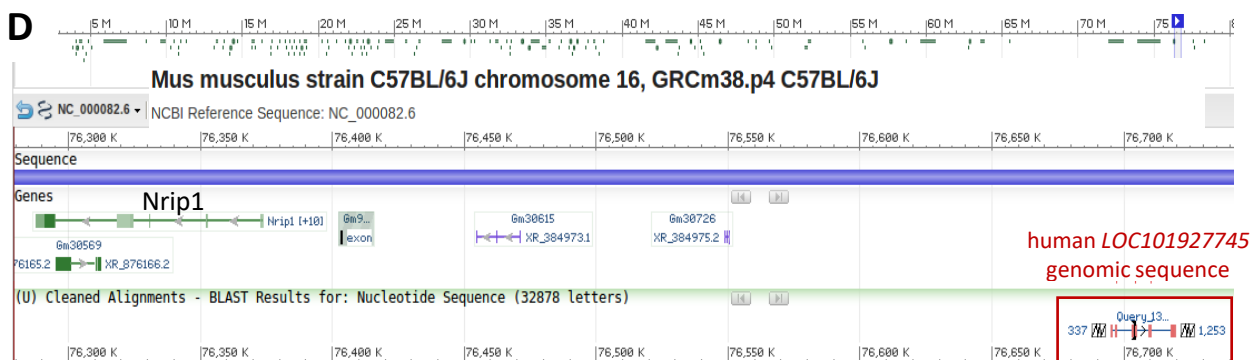
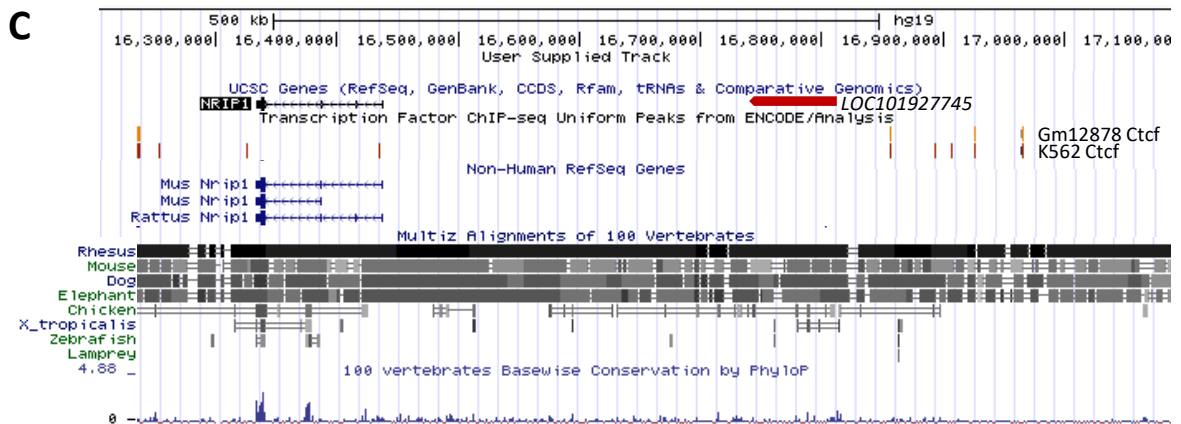
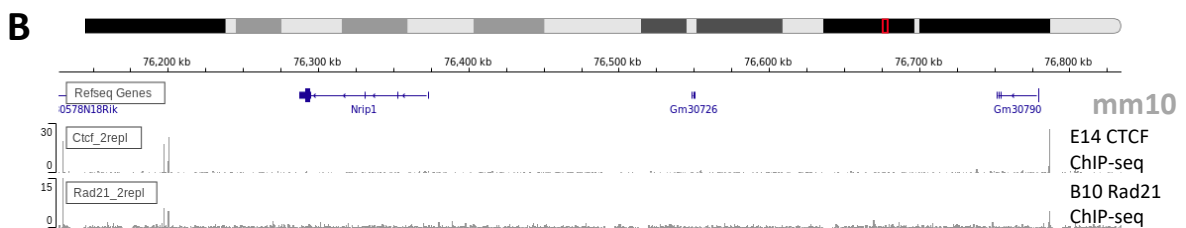
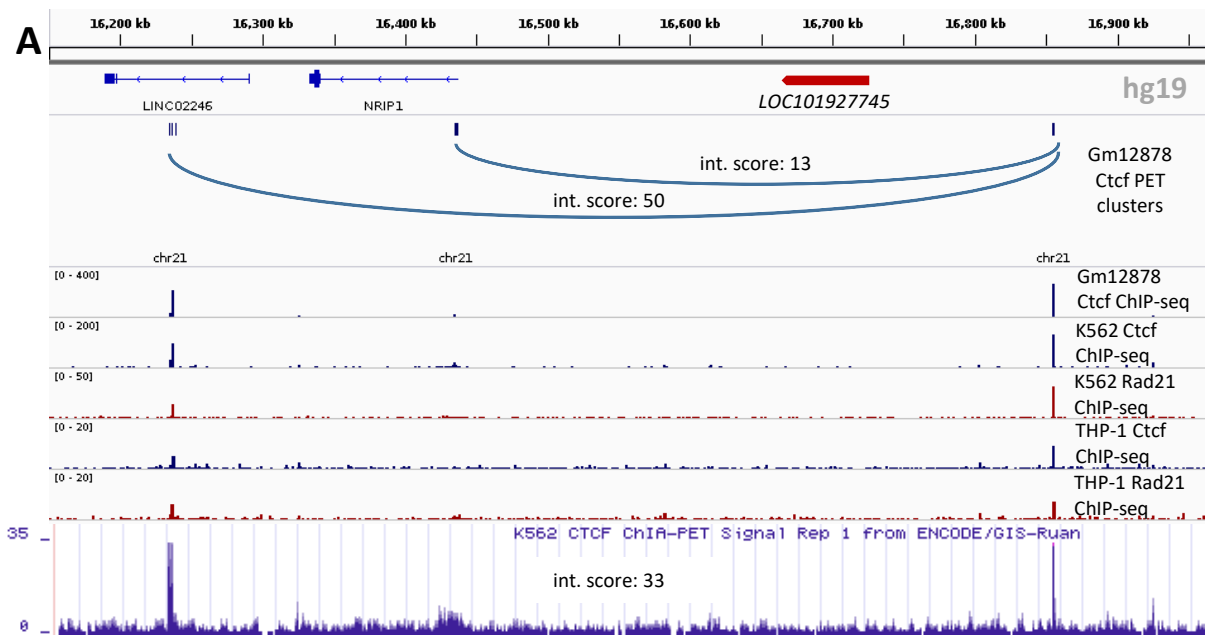


Figure S3.

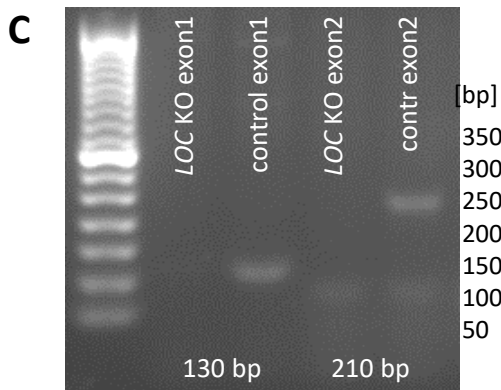
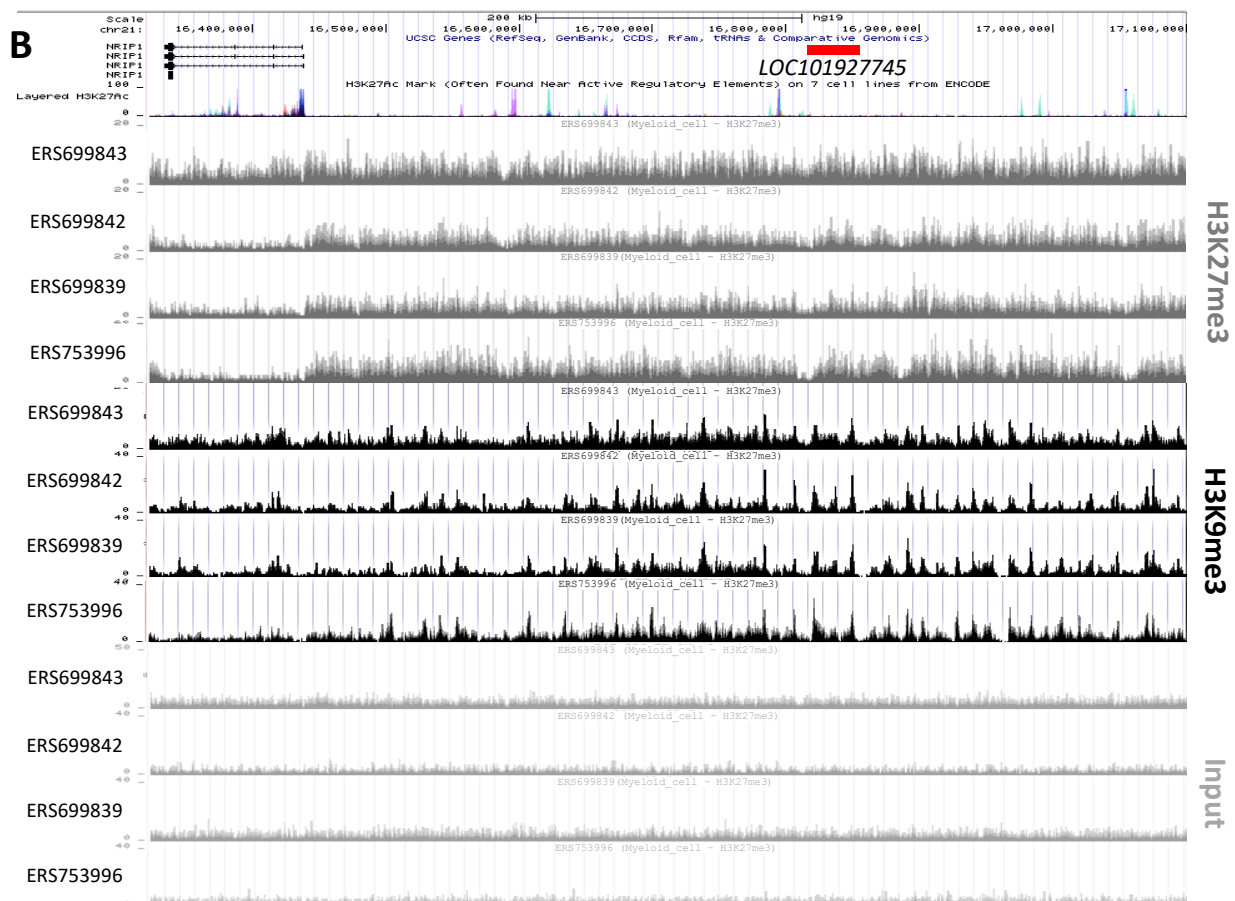
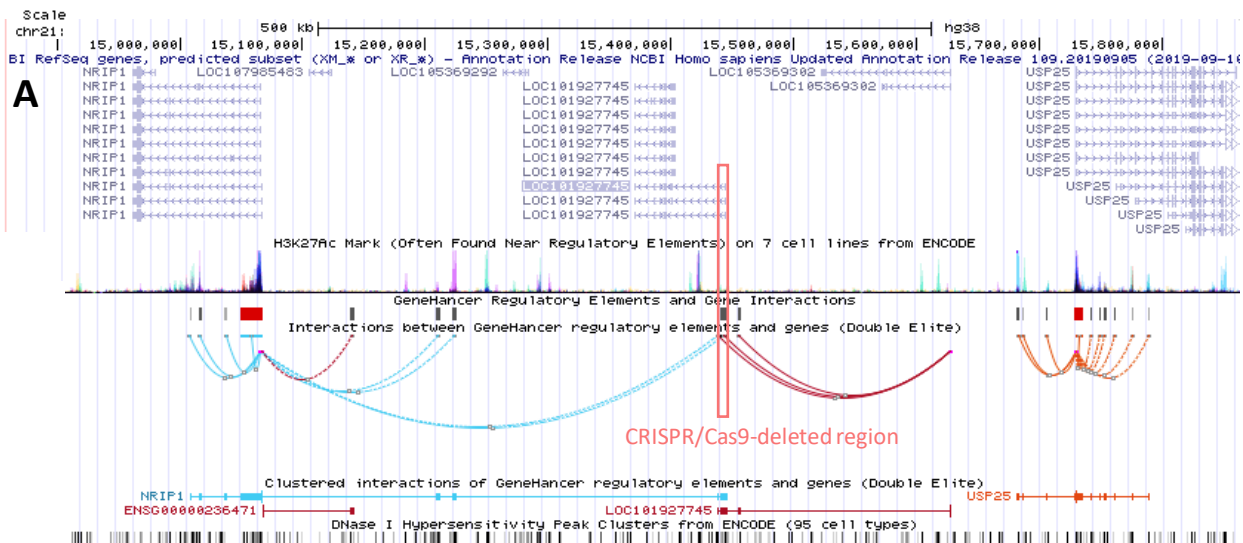


Figure S4.



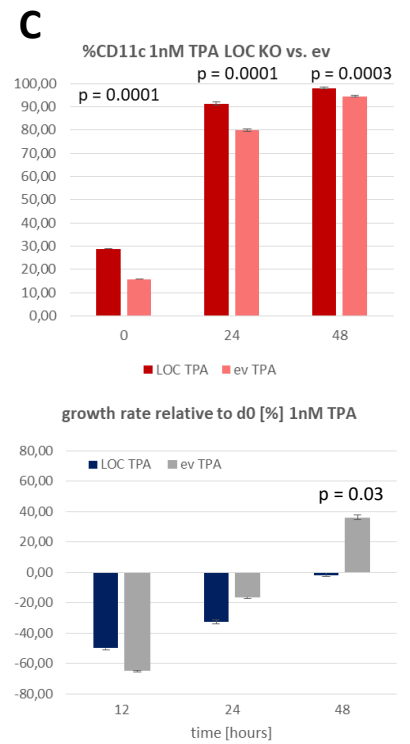
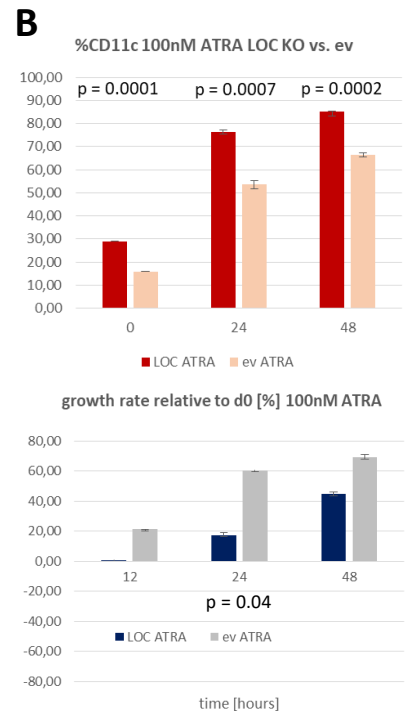
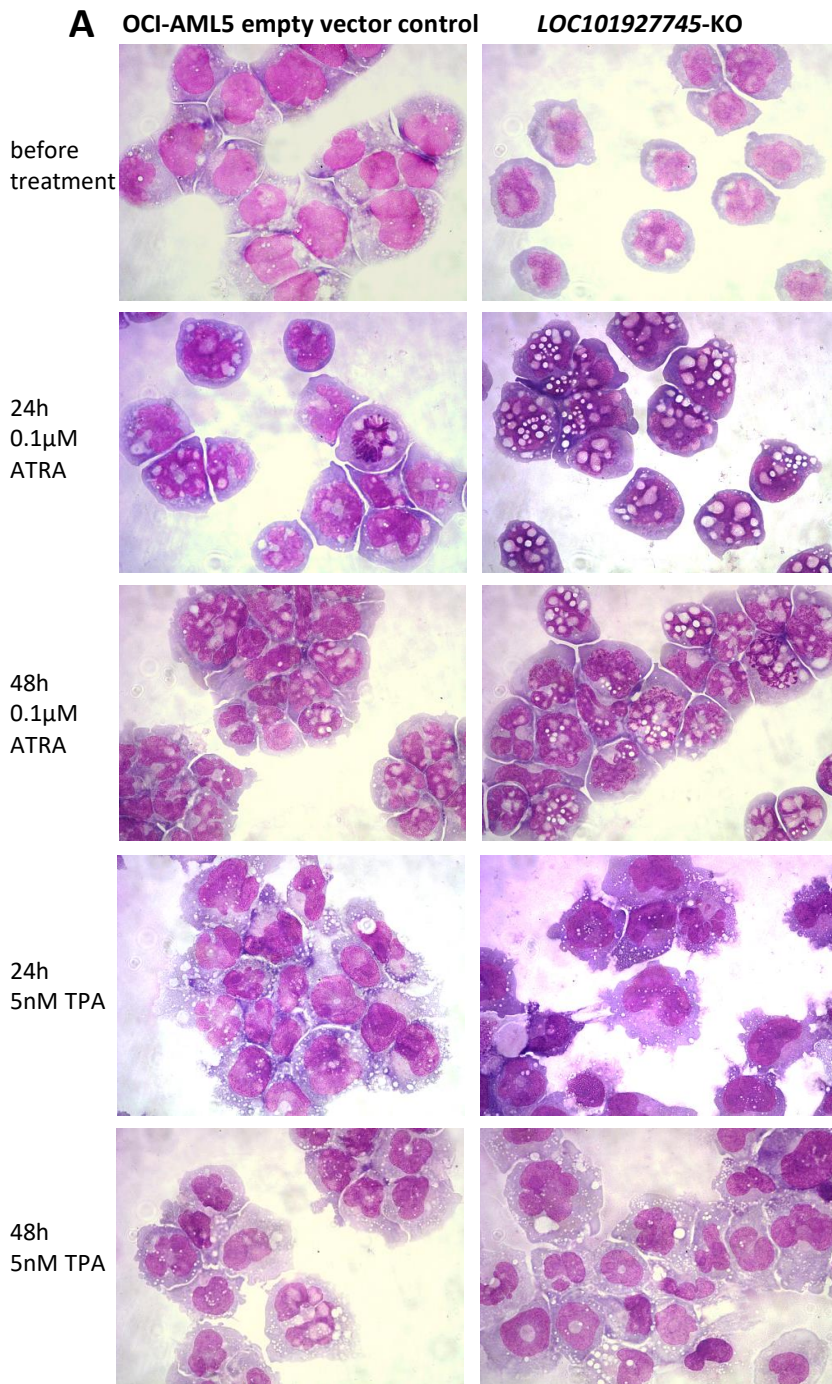
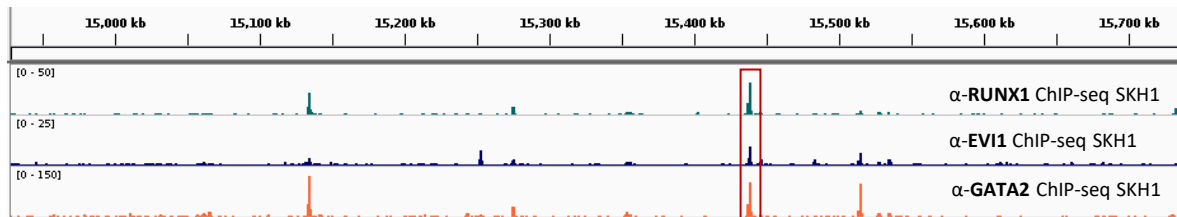


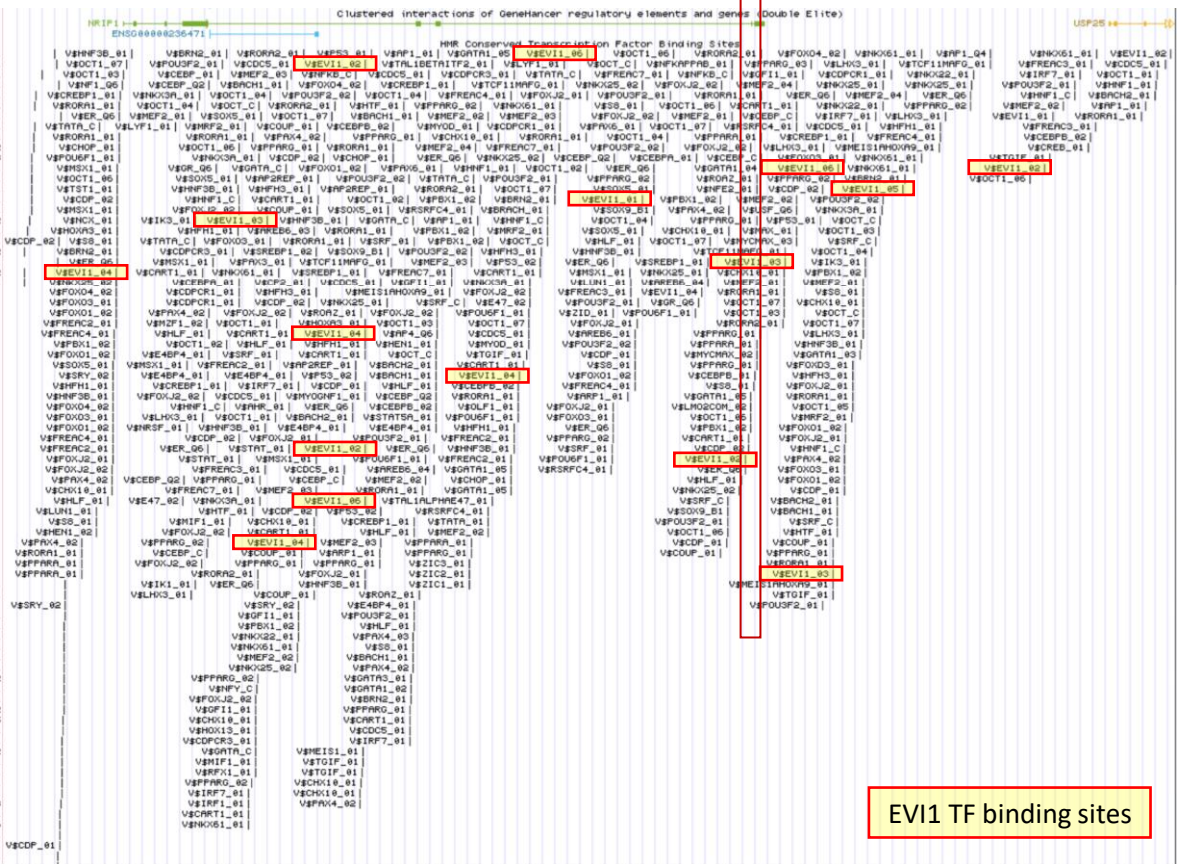
Figure S5.

**A**



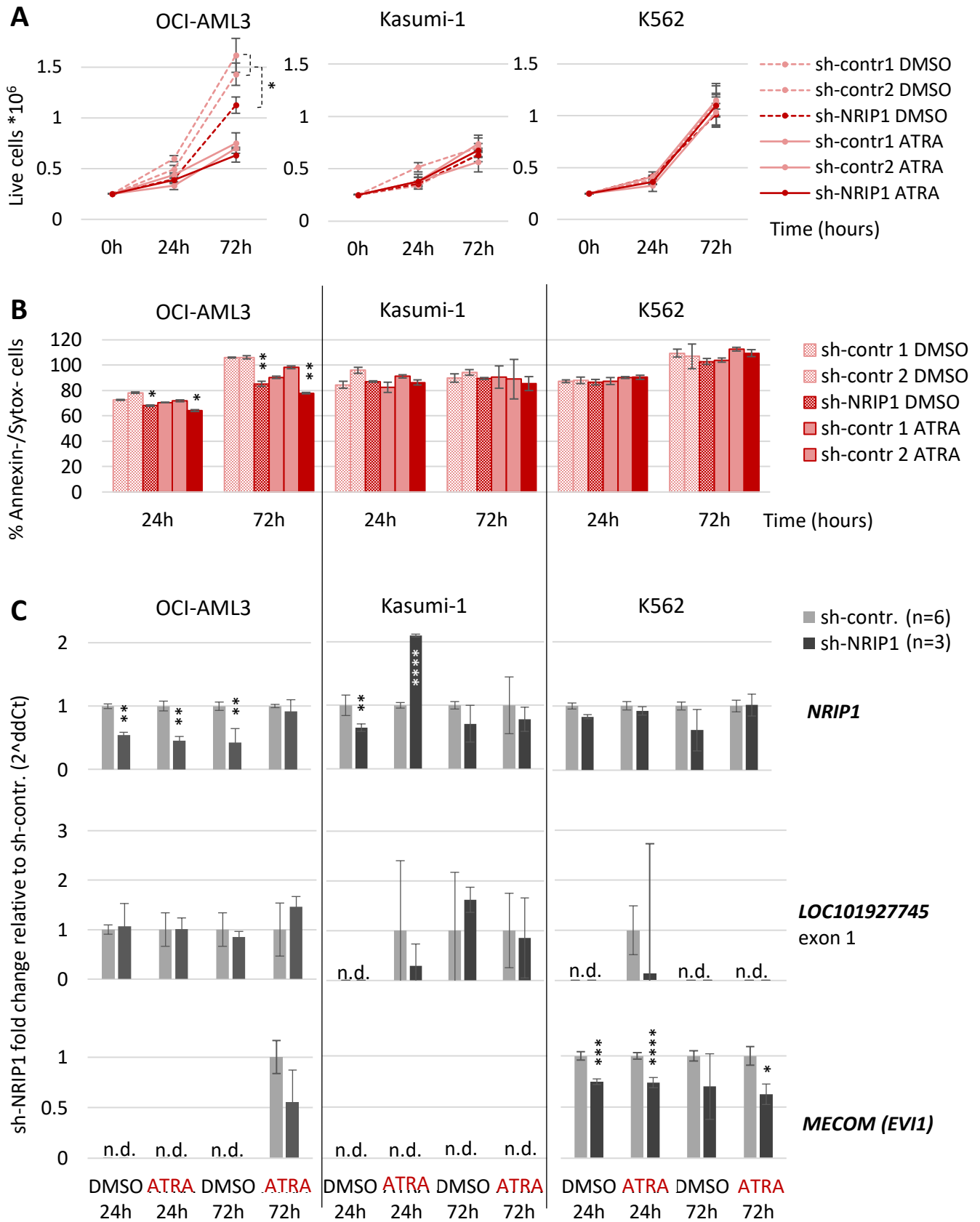
*GH21J015439*

**B**



EVI1 TF binding sites

**Figure S6.**



\* $p < 0.01$ , \*\* $p < 0.001$ , \*\*\* $p < 0.0001$ , \*\*\*\* $p < 0.00001$

Figure S7.

## OCI-AML3

## Kasumi1

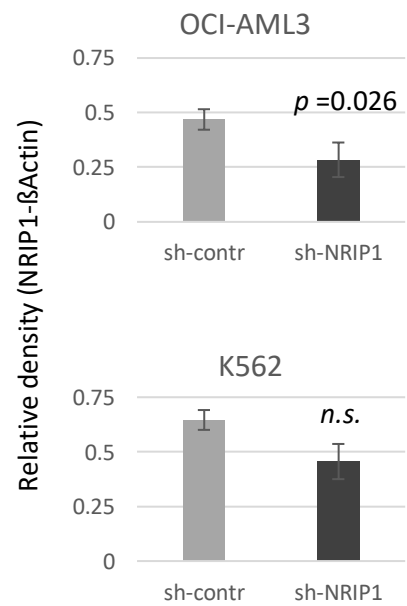
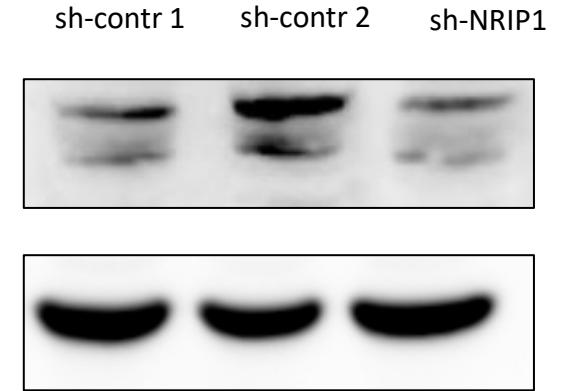
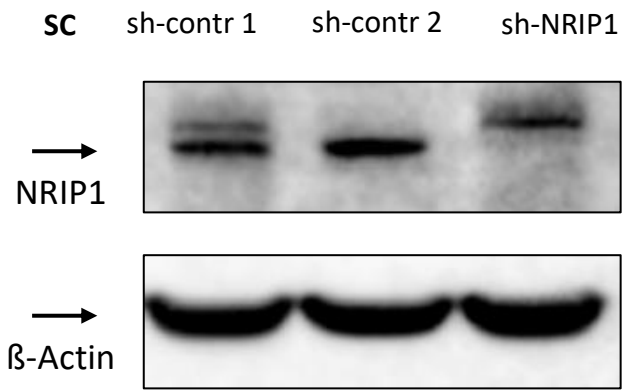


Figure S8.

## UCSD-AML1

## HNT-34

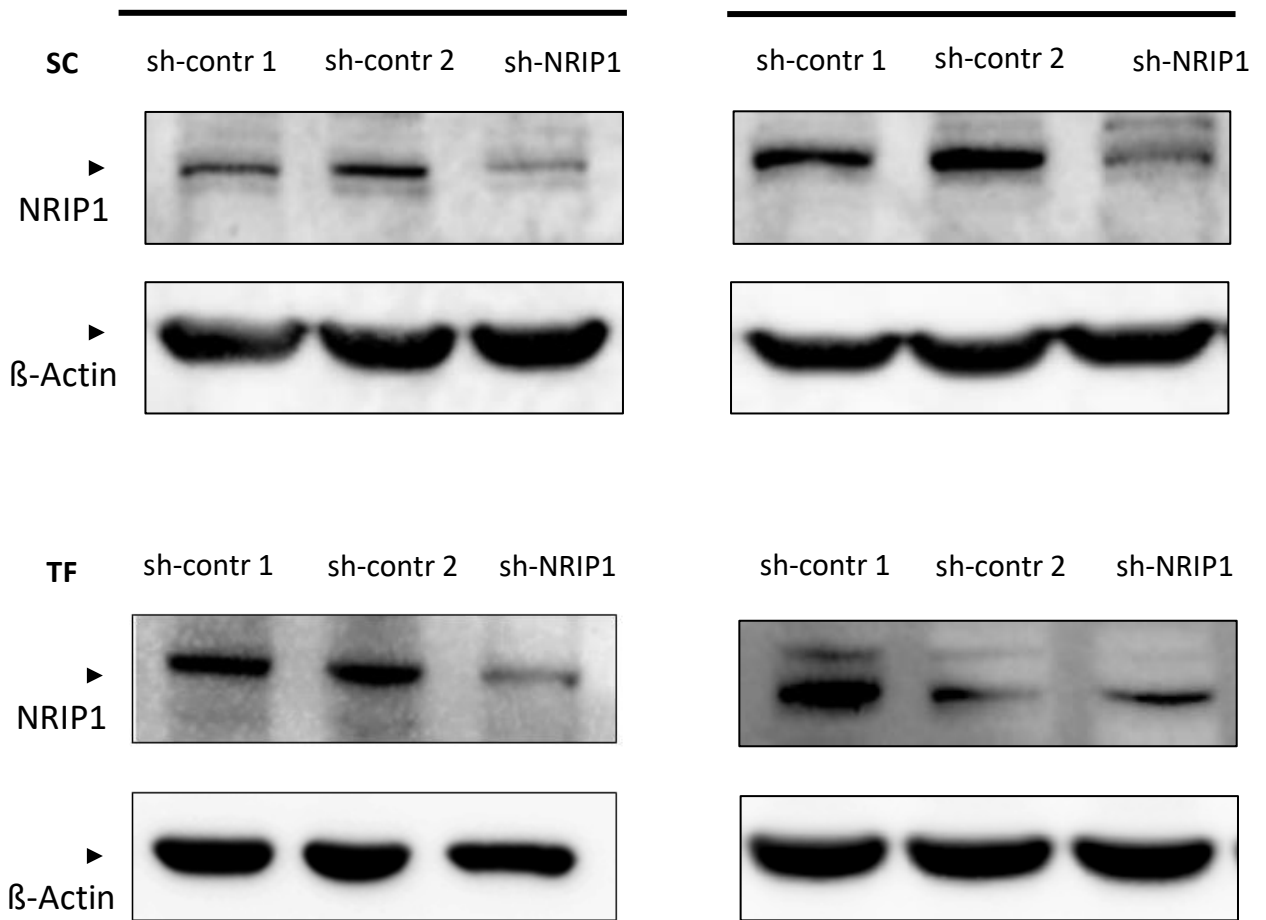
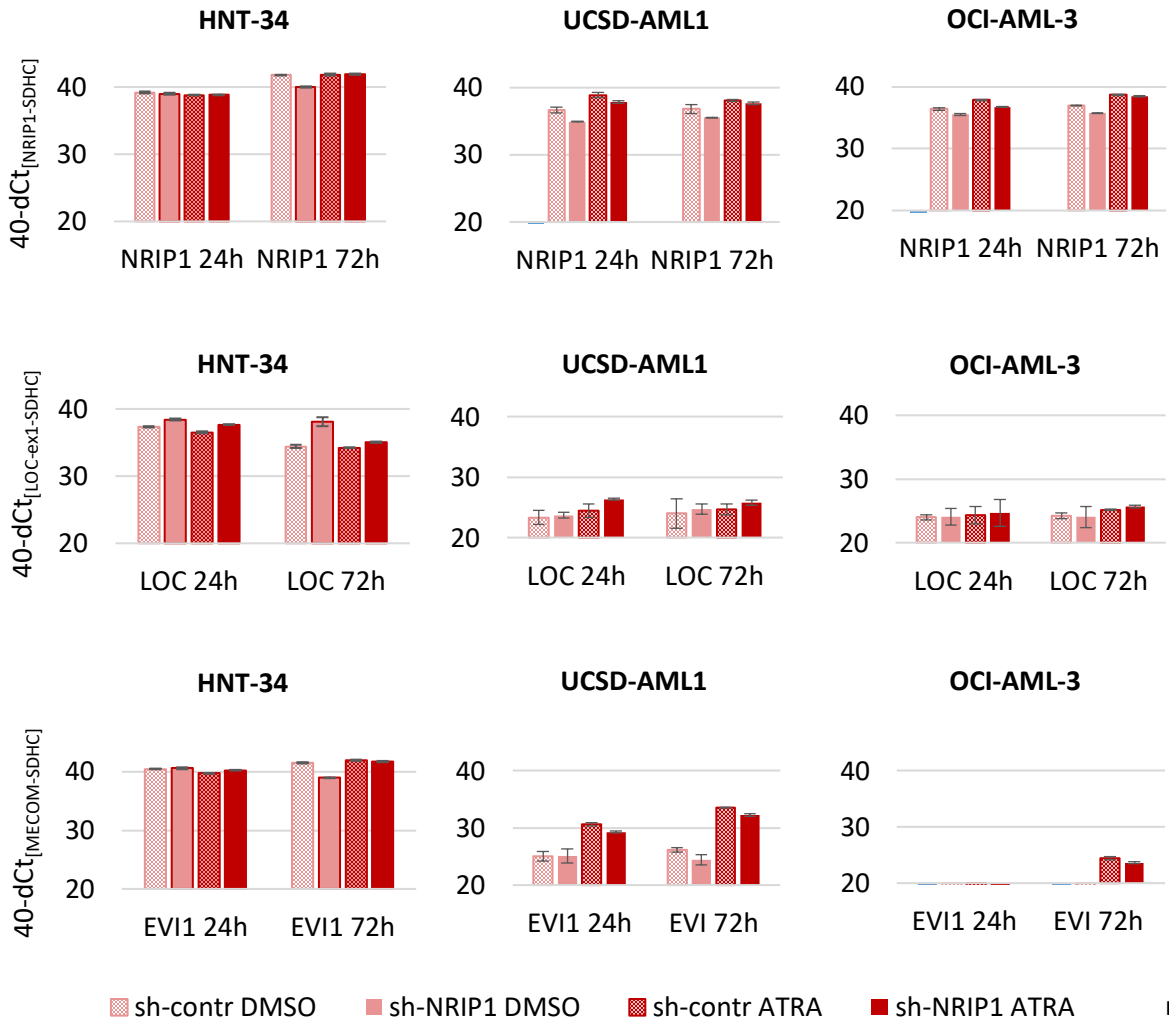


Figure S9.



**TTEST HNT-34 (DMSO vs ATRA)**

	<i>NRIP1</i>	<i>LOC</i>	<i>EVI1</i>
sh-contr 24h	0.0926	<b>0.0001</b>	<b>0.0000</b>
sh-NRIP1 24h	<b>0.0411</b>	<b>0.0062</b>	<b>0.0103</b>
sh-contr 72h	0.8315	0.4749	<b>0.0284</b>
sh-NRIP1 72h	<b>0.0124</b>	<b>0.0000</b>	<b>0.0000</b>

**TTEST HNT-34 (sh-contr vs sh-NRIP1)**

	<i>NRIP1</i>	<i>LOC</i>	<i>EVI1</i>
DMSO 24h	0.7534	<b>0.0008</b>	0.1030
ATRA 24h	0.6176	<b>0.0000</b>	<b>0.0001</b>
DMSO 72h	<b>0.0000</b>	<b>0.0014</b>	<b>0.0000</b>
ATRA 72h	0.7003	<b>0.0001</b>	<b>0.0127</b>

**TTEST UCSD-AML1 (DMSO vs ATRA)**

	<i>NRIP1</i>	<i>LOC</i>	<i>EVI1</i>
sh-contr 24h	<b>0.0005</b>	0.2910	<b>0.0011</b>
sh-NRIP1 24h	<b>0.0002</b>	<b>0.0036</b>	<b>0.0093</b>
sh-contr 72h	0.0535	0.1440	<b>0.0008</b>
sh-NRIP1 72h	0.0675	0.2702	<b>0.0103</b>

**TTEST UCSD-AML1 (sh-contr vs sh-NRIP1)**

	<i>NRIP1</i>	<i>LOC</i>	<i>EVI1</i>
DMSO 24h	<b>0.0004</b>	0.6162	0.9082
ATRA 24h	<b>0.0104</b>	0.0392	<b>0.0011</b>
DMSO 72h	0.0592	0.2410	0.1242
ATRA 72h	0.0675	0.5547	<b>0.0013</b>

**TTEST OCI-AML3 (DMSO vs ATRA)**

	<i>NRIP1</i>	<i>LOC</i>	<i>EVI1</i>
sh-contr 24h	<b>0.0003</b>	0.6099	NA
sh-NRIP1 24h	0.0540	0.9940	NA
sh-contr 72h	<b>0.0003</b>	0.8479	<b>0.0110</b>
sh-NRIP1 72h	<b>0.0360</b>	0.2958	<b>0.0063</b>

**TTEST OCI-AML3 (sh-contr vs sh-NRIP1)**

	<i>NRIP1</i>	<i>LOC</i>	<i>EVI1</i>
DMSO 24h	<b>0.0007</b>	0.912	NA
ATRA 24h	<b>0.0025</b>	0.858	NA
DMSO 72h	<b>0.0000</b>	0.606	NA
ATRA 72h	0.0360	<b>0.022</b>	0.066

**Figure S10.**

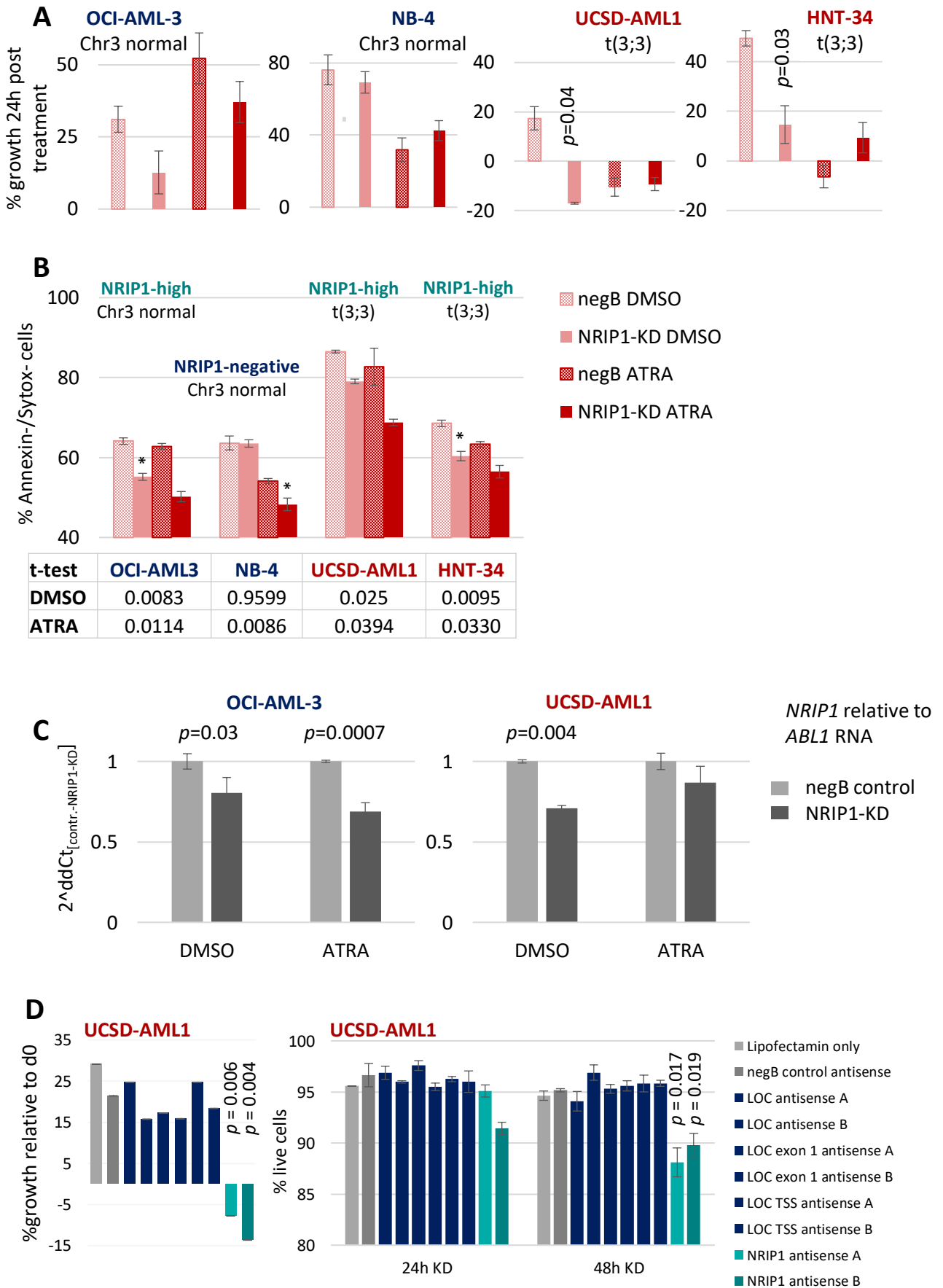


Figure S11.

## Supplementary Material and Methods

### 1) Sequencing of CK-AML samples

RNA Sequencing was performed on primary complex karyotype (CK-AML) patient samples (n=65) from viably frozen BM. The definition of CK-AML followed the recommended criteria<sup>1</sup> and diagnosis of AML was based on French-American-British Cooperative Group and WHO criteria for cases diagnosed after 2004. 40/65 (62%) patients were treated on consecutive multicenter treatment trials of the AML Study Group (AMLSG) applying age-adjusted intensive chemo-therapy: AMLHD98A (n=4; NCT00146120) and AMLSG07-04 (n=22; NCT00151242) for younger patients (16 to 60 years); AMLSG06-04 (n=14; NCT00151255) for elderly patients (>60 years)<sup>1</sup>. All studies were approved by local ethics committees, and all patients gave informed consent for treatment, cryopreservation of samples, and molecular analyses according to the Declaration of Helsinki. RNA libraries were prepared from 1µg of total input RNA (RNeasy Mini Kit, Qiagen, The Netherlands) using the TruSeq v2 LS Poly-A enriched RNA Preparation Kit with Ribo-Zero Human/Mouse/Rat (Illumina, San Diego, CA, USA) according to the manufacturer's instructions and were sequenced on an Illumina HiSeq2000 at the Stanford Sequencing Service Center, CA, USA (100bp, paired-end) yielding an average of 148 (±31)×10<sup>6</sup> reads per sample. Low quality bases (Phred < 20) and adapters were removed from the Fastq raw reads using Trimmomatic v0.38 (ref<sup>2</sup>) and read quality was assessed using FastQC v0.10.1 (available at [www.bioinformatics.babraham.ac.uk](http://www.bioinformatics.babraham.ac.uk)). Cleaned-up reads were aligned to the human reference genome GRCh38 release 23 using STAR v2.4 (ref<sup>3</sup>) and subsequently sorted and indexed using *samtools* v0.1.19 (ref<sup>4</sup>). Alignment quality statistics and count matrices were computed using *HTSeq*<sup>5</sup>. All uniquely aligned reads that were unambiguously assigned to annotated features (Gencode v23 ALL superset) were normalized and transformed using the *R* packages *edgeR* v3.18.1 (ref<sup>6</sup>) and *limma*<sup>7</sup>. Gene fusions were called using multiple independent algorithms (as paired reads that flank, or single-reads that span fusion junctions). Identified gene fusions were independently validated by long range PCR followed by nanopore sequencing on a MinION Flowcell R9 (Oxford Nanopore Technology, Cambridge, UK). Data from the CK-AML dataset will be made available through the corresponding author upon reasonable request.

### 2) CRISPR/Cas9-mediated LOC101927745 knock-out

OCI-AML-5 cells that had been transduced with a Cas9-ORF-carrying DHC013 vector and selected with 5µg/mL Blasticidin were kindly provided by Dr. Jan Krönke (Ulm University Hospital, Germany). Cas9-expression was confirmed via Western Blot. sgRNAs targeting the *LOC101927745* TSS were designed using the design suite CCTop (available at: <https://crispr.cos.uni-heidelberg.de/>):

T1:                                   5'-CACCGCTGCCACAGAACGATGACAC-3'fw,  
  5'-AAACGTGTCATCGTTCTGTGGCAGC-3'rev,  
T2:                                   5'-CACCGATTATTGCTAAGGTGCATCT-3'fw,  
  5'-AAACAGATGCACCTTAGCAATAATC-3'rev.

Each sgRNA pair was cloned into either *pL40C-CRISPR.EFS.PAC* or *pL-CRISPR.EFS.tRFP*, respectively (kindly provided by Dr. Dirk Heckl at Martin-Luther-University in Halle, Germany), both with the Cas9-ORF removed. 1\*10<sup>6</sup>cells/mL were spin-infected with an equimolar mix of virus-containing medium +10mg/mL Polybrene, then single cell clones were sorted, expanded in 1µg/mL Puromycin, and sent for Sanger sequencing. Lack of expression from the deleted site and additional exons was confirmed in homozygous knock-out (KO) and control cell lines via RT PCR (PlatinumTaq, ThermoFisher Scientific) and qRT-PCR (TBgreen, TaKaRa Bio Inc., Japan) using 10 different primer sets in total. PCR results shown in **Supplementary Figure S4C** used primers for exon 1B and exon 2.



### **3) *GapmeR-mediated knock-down of NRIP1 mRNA and LOC101927745 transcript***

Three Antisense LNA GapmeRs (Qiagen, The Netherlands) were assessed for optimal knockdown of the target gene and the most effective GapmeR was titrated and utilized at a 50nM concentration according to the manufacturers' instructions.  $2.0 \times 10^6$  t(3;3) USCD-AML1 or OCI-AML3 cells/mL were treated in triplicates with either NRIP1-targeting FAM-labeled antisense GapmeRs, 3 different sets of *LOC101927745*-targeting GapmeRs, a non-target GapmeR control ("NegB", Qiagen, The Netherlands) or with transfection agent alone (Lipofectamine 2000, ThermoFisher Scientific, USA). Transfection efficiency was determined via flow cytometry and nuclear localization was confirmed via fluorescence microscopy. Knock-down efficiency was determined via qPCR for both products and for protein levels of NRIP1 vs ACTIN.

### **4) *shRNA-mediated knock-down of NRIP1 mRNA***

Five short hairpin RNAs (shRNAs) targeting *NRIP1* mRNA (TRCN0000019779-TRCN0000019783) as well as 2 different control sequences (TRCN0000060640, TRCN0000060668) each in a pLKO.1 vector backbone, were purchased from the RNAi Consortium (TRC) library (University of British Columbia, Canada, and separately lipofected into 293T-LentiX cells at 3ug with 1.8ug psPAX2 + 300ng pMD2.G using Lipofectamine 2000 (ThermoFisher Scientific, USA) according to manufacturer's protocol. Lentiviral supernatants for all shRNAs as well as a non-targeting mammalian scrambled control were harvested and used to infect  $0.3 \times 10^6$  UCSD-AML1 or OCI-AML3 cells via spin infection at 380 x g for 1 hour, followed by overnight incubation. Transformed cells were selected with 2ug/mL puromycin (STEMCell Technologies, Canada) for 10 days. The shRNA resulting in the strongest NRIP1 RNA knockdown (TRCN0000019782, DNA sequence: GCTGCAAGATTACAGGCTGTT) was selected for all further functional investigation.

### **5) *Quantitative Real-Time PCR***

Total RNA was extracted (RNeasy Mini Kit, Qiagen, The Netherlands), on-column DNase-digested and reverse-transcribed to cDNA (TaKaRa Bio Inc., Japan). Quantitative PCR was performed in technical triplicates using SYBR green chemistry (TBgreen, TaKaRa Bio Inc., Japan) with subsequent melting curve analysis for *LOC101927745* and TaqMan probe assays for *NRIP1* (ThermoFisher Scientific, USA). Delta Ct (dCt) values were calculated relative to the pre-determined housekeeping genes encoding *Abelson murine leukemia viral oncogene homolog 1 (ABL1)* and *Succinate Dehydrogenase Complex Subunit C (SDHC)*. A list of primers is included below.

### **6) *NRIP1 protein quantification (Western Blot)***

Protein pellets were dissolved in 5% SDS in PBS with proteinase inhibitor and quantified via bicinchoninic acid (BCA) protein assay. Expression levels were assessed via enzyme-linked immunosorbent assay *via* Western blot using Anti-RIP140 (NRIP1) (F-2) primary antibody (Santa Cruz Biotechnology, USA).

### **7) *Statistics***

All tests of significance for were performed at 95% confidence after testing for distribution and adjusted for multiple hypothesis testing when appropriate as indicated in the Figure legends for each respective analysis. All shown error bars represent standard deviations (SD). SD for fold changes were calculated as  $\sqrt{SD_{\text{sample1}}^2 + SD_{\text{sample2}}^2}$ . Fold changes were determined using the  $2^{\text{dCt}}$  method for qRT-PCR data and *via* calculation of  $\log_2(\text{ratio}-1)$  for sequencing data.

## PCR primer sequences for *LOC101927745*

Exon1A) 5'-agcttccccagcattcaagt-3'fw,  
5'-gcacactgccatcctcaatg-3'rev  
exon1B) 5'- ATGGAAGGCAGAATAGCGCA-3'fw,  
5'- TGGAAGTGGACTTCAAAGCA-3'rev  
exon2) 5'-AAAGAAGCCGCCAGAGAAGAT-3'fw,  
5'-ACAGAACGATGACACAGGGA-3'rev  
exon 10) 5'- CCTCTGTGGCTTGTTCCT-3'fw,  
5'- AAAGAGCAACCGAACCGTCA-3'rev

## References used in Supplement

1. Rucker FG, Schlenk RF, Bullinger L, Kayser S, Teleanu V, Kett H *et al.* TP53 alterations in acute myeloid leukemia with complex karyotype correlate with specific copy number alterations, monosomal karyotype, and dismal outcome. *Blood*. **2012**, 119, 2114–2121.
2. Bolger AM, Lohse M, Usadel B. Trimmomatic: A flexible trimmer for Illumina Sequence Data. *Bioinformatics*. **2014** btu170.
3. Dobin A, Davis CA, Schlesinger F, Drenkow J, Zaleski C, Jha S, *et al.* *Bioinformatics*. **2013** Jan 1;29(1):15-21.
4. Li H, Handsaker B, Wysoker A, Fennell T, Ruan J, Homer N, *et al.* The Sequence alignment/map (SAM) format and SAMtools. *Bioinformatics* **2009**, 25, 2078-9.
5. Anders S, Pyl PT, Huber W. HTSeq--a Python framework to work with high-throughput sequencing data. *Bioinformatics*. **2015** Jan 15;31(2):166-9.
6. McCarthy DJ, Chen Y, Smyth GK. Differential expression analysis of multifactor RNA-Seq experiments with respect to biological variation. *Nucleic Acids Research*. **2012**, 40, 4288-4297.
7. Diboun I, Wernisch L, Orengo CA, Koltzenburg M. Microarray analysis after RNA amplification can detect pronounced differences in gene expression using limma. *BMC Genomics*. **2006** Oct 9;7:252.